PHYSICAL REVIEW A VOLUME 25, NUMBER 2 FEBRUARY 1982

Hidden structure in liquids

Frank H. Stillinger and Thomas A. Weber
Bell Laboratories, Murray Hill, New Jersey 07974
(Received 24 August 1981)

The canonical partition function for classical many-body systems is transformed so that the temperature-independent packing statistics and the thermal excitations are uniquely separated. This requires classification of particle configurations according to multidimensional potential-energy minima that can be reached by steepest-descent paths ("quenches"). Such classifications have been constructed for several starting configurations in the solid, fluid, and coexistence phases of the two-dimensional Gaussian core model. These quenches reveal a remarkable degree of polycrystalline order hidden within the fluid phase by "vibrational" distortion, and that order appears to have a large correlation length. The results suggest that melting hinges upon defect softening in the quenched packings, and a crude "theory" of melting for the Gaussian core model is developed in the Appendix.

I. BACKGROUND

The melting of crystalline solids causes configurational regularity at the molecular level to be replaced by substantial disorder. This change is vividly revealed by x-ray- or neutron-diffraction experiments wherein Bragg reflections characteristic of the crystal disappear. No less vivid is the huge increase in the self-diffusion constant upon melting, which depends upon the diversity of packing structures available to molecules in the liquid (compared to the crystal) and the ease of transition between those structures.

The present paper follows the long tradition of attempting to bring conceptual order to the disordered liquid state. The key feature introduced in this approach is a configurational mapping whereby arbitrary sets of molecular positions are referred, essentially uniquely, to relative minima on the potential-energy hypersurface for the many-body system.[1] This mapping is generated by a quenching operation that follows steepest-descent paths on the hypersurface; details appear in Sec. II.

The configurational mapping separates the statistical-mechanical description of the many-body system fundamentally into two distinct parts. In loose terminology these are the mechanically stable packing part (all particles free of net force and torque), and the vibrational part. Temperature appears explicitly only in the latter. Section III shows how this separation causes the canonical partition function to transform formally from a multidimensional integral over all configurational coordinates to a one-dimensional integral over potential energy. This new partition function representation is convenient in some respects for understanding the melting transition itself, as later remarks indicate.

We have carried out portions of this general program by specific numerical calculations on the Gaussian core model[2,3] in two dimensions.[4] Results are displayed and discussed in Sec. IV. By undertaking the quenching operation from several initial thermodynamic states we seem to have established that a remarkable polycrystalline order lies hidden in the fluid phase, heavily obscured from view in the thermodynamic state by the distracting influence of vibrations. Not surprisingly, the quenching out of these vibrations causes the pair-correlation functions to sharpen and to restructure in a manner consistent with that polycrystalline order. Barring the possibility of "hexatic" phases[5,6] as the initial starting point, we believe that the hidden polycrystalline order is not peculiar to the Gaussian core model but would be revealed for any two-dimensional system with central pair potentials.

The idea of resolving observable order in liquids into a vibrational part and an inherent structural part is not new. It certainly underlies the study of pair-correlation functions evaluated from time-averaged particle positions in computer simulations using molecular dynamics.[7,8] It also underlies the experimental strategy that examines low-

temperature amorphous ice for clues to hydrogen bond order in liquid water.[9] From an unremittingly theoretical viewpoint the present quenching procedure seems to be the most straightforward option, and it is free of arbitrariness such as coordinate averaging times.

The specific results obtained for the Gaussian core model suggest a simple view of two-dimensional melting that is explored in the Appendix. While the calculation offered there is admittedly crude, it suggests (we believe correctly) that the first-order melting process depends fundamentally on softening of the regular crystal by disorder.

II. CONFIGURATIONAL MAPPING

We consider a set of N molecules confined to a fixed containment region V. For present purposes it is irrelevant whether containment results from specific wall forces or by imposition of periodic boundary conditions. For each molecule $1 \leq j \leq N$, the vector $\vec{r}_j$ will give the configurational coordinates; if j contains ν nuclei and D is the space dimension $\vec{r}_j$ will possess νD components.

Let $\Phi(\vec{r}_1, \ldots, \vec{r}_N)$ denote the system potential-energy function. It will, in general, include intramolecular bond potentials, intermolecular interactions, and wall potentials (if any). We will suppose that Φ is bounded and differentiable for all configurations $\vec{r} \equiv \vec{r}_1, \ldots, \vec{r}_N$ not involving coincidence of nuclei.

Within the purview of classical mechanics the time evolution of the system (in mass-reduced time units) normally follows the Newtonian equations

$$\ddot{\vec{r}} = -\nabla\Phi \, . \tag{2.1}$$

We shall be concerned instead with the corresponding *first-order* evolution equations

$$\dot{\vec{r}} = -\nabla\Phi \, , \tag{2.2}$$

which describe steepest-descent paths on the multidimensional Φ hypersurface. Excepting certain unimportant cases with zero measure, Eq. (2.2) connects any starting point $\vec{r}$ in the configuration space uniquely to a local minimum of Φ. By this means we generate a mapping $M(\vec{r})$ from the continuum $\vec{r}$ onto the discrete set of minima which can be indexed by α:

$$M(\vec{r}) = \alpha \, . \tag{2.3}$$

The steepest-descent paths are limiting solutions for the Newtonian equations (2.1) augmented by a first-order damping term with very large damping constant. It is appropriate to view the corresponding dissipative motion as a quench since both kinetic and potential energy are being removed until the system comes to rest. In the large damping limit [i.e., Eq. (2.2)] the quench is so effective that the system is never able to surmount a potential-energy barrier. Instead, the system is forever trapped in the neighborhood of the same relative minimum α where it found itself at the beginning of the quench. Since no annealing (barrier hopping) is possible during the course of steepest descents, the mapping M can informally be regarded as the operation of an infinitely rapid quench to absolute zero temperature.

Let $R(\alpha)$ denote the set of system configurations $\vec{r}$ which quench to local minimum α; that is, the region in the νDN-dimensional configuration space which satisfies mapping (2.3) for given α. Obviously, each $R(\alpha)$ is connected, for any two points in its interior are each connected to the minimum α and, therefore, to one another by a path within $R(\alpha)$. We cannot say under general circumstances that the $R(\alpha)$ are convex. Indeed, it may happen that they are multiply connected, though that can occur only if a saddle point exists within the interior of $R(\alpha)$ at which the quench paths bifurcate.

Boundaries separating distinct quench regions are $(\nu DN\text{-}1)$-dimensional hypersurfaces. Their union constitutes the zero measure set of system configurations for which mapping M is undefined.

Many pairs of mechanically stable particle packings will be identical except for particle permutation. For conceptual simplicity it makes sense to group packings and their associated quench regions into equivalence classes. We can write the number of members in any such equivalence class as $N!/\sigma$. The symmetry number σ will be unity for all packings that are rigidly confined by wall forces. By contrast, periodic boundary conditions permit free translation of packings that for a periodic crystalline array allow any one particle to be moved to the position of any other without changing Φ, and for this case $\sigma = N$. Yet other circumstances can be devised for which σ would lie between these extreme values 1 and N.

III. TRANSFORMED PARTITION FUNCTION

The canonical partition function for N structureless particles at inverse temperature $\beta = 1/k_B T$ is

$$Z_N = (\lambda^{DN} N!)^{-1} \int \exp[-\beta\Phi(\vec{r})] d\vec{r} \, . \tag{3.1}$$

Here, λ is the mean thermal de Broglie wavelength. We shall now transform Z_N from this conventional representation to a less familiar but conceptually useful alternative, based on the considerations of Sec. II.

First, we break the configurational integral in Eq. (3.1) into separate contributions from each of the quench regions $R(\alpha)$:

$$Z_N=(\lambda^{DN}N!)^{-1}\sum_{\alpha}\int_{R(\alpha)}\exp[-\beta\Phi(\vec{r})]d\vec{r}\ . \tag{3.2}$$

As remarked earlier, it is convenient to treat together members of $R(\alpha)$ equivalence classes. If we select one quench region from each equivalence class to sum over (indicated by a primed summation) then Eq. (3.2) is trivially modified to the following:

$$Z_N=\lambda^{-DN}\sum_{\alpha}'[\sigma(\alpha)]^{-1}\int_{R(\alpha)}\exp[-\beta\Phi(\vec{r})]d\vec{r}\ . \tag{3.3}$$

Within any region $R(\alpha)$ we can write

$$\Phi(\vec{r})=\Phi_\alpha+\Delta_\alpha\Phi(\vec{r})\ , \tag{3.4}$$

where Φ_α is the value of the potential-energy function at local minimum α, and the non-negative quantity $\Delta_\alpha\Phi$ measures potential energy from that minimum. Consequently,

$$Z_N=\lambda^{-DN}\sum_{\alpha}'[\sigma(\alpha)]^{-1}\exp(-\beta\Phi_\alpha)\times\int_{R(\alpha)}\exp[-\beta\Delta_\alpha\Phi(\vec{r})]d\vec{r}\ . \tag{3.5}$$

Notice that the evaluation of Z_N here has been separated into two parts, namely, the identification of all distinct (temperature-independent) packings, and the thermal excitation of each of those packings within their own regions $R(\alpha)$.

The most effective way to describe the large system limit utilizes the potential energy per particle ϕ as the basic variable. Insofar as the mechanically stable packings are concerned the system will have its potential per particle confined between finite limits:

$$\phi_0\le\phi\le\phi_u\ . \tag{3.6}$$

The lower limit corresponds to the ordered crystal that has absolute stability at zero absolute temperature. At the other extreme there exists presumably some "worst" packing that puts particles in a mechanically stable configuration with ϕ_u as the potential per particle. The vast majority of packings lie between these extremes with some distribution of ϕ values which we will denote by $G(\phi)$, a density of packing states along the ϕ axis. It should be kept in mind that this density of states enumerates only *distinct* packings, i.e., packing equivalence classes. Obviously, we have the following formal expression:

$$G(\phi)=\sum_{\alpha}'\delta(\phi-\Phi_\alpha/N)/\sigma(\alpha)\ . \tag{3.7}$$

In the event that the total potential energy $\Phi(\vec{r})$ is composed of short-range particle interactions it is reasonable to suppose that conversions from one packing to another could be effected by sequences of localized particle rearrangements. If a very large system were imagined subdivided into cells, each large compared to the particle neighbor spacing, then rearrangements within each cell could largely be carried out independently of those in the other cells. The overall number of packings could then be reckoned as multiplicative over the cells, at least in leading order. One thus concludes that for large N the total number of distinguishable packings (equivalence classes) should be exponential in N. A more accurate version of this argument would account for interactions between neighboring cells, but since the effect of such interactions loses relative importance as cell size increases, it seems difficult to avoid the same conclusion that the total number of distinguishable packings rises exponentially with increasing N at fixed density.

We take this last result to indicate that the density-of-states function $G(\phi)$ likewise is essentially exponential in N. First, understanding that some suitable coarse graining is applied to smooth out the Dirac δ functions appearing in Eq. (3.7), we write for large N,

$$\ln G(\phi)\sim Ng(\phi)\ . \tag{3.8}$$

It seems reasonable to suppose that $g(\phi)$ is at least continuous within the interior of the interval (3.6), and that rarity of possible packings near the endpoints of that interval requires

$$\lim_{\phi\to\phi_0}g(\phi)=-\infty\ ,\qquad \lim_{\phi\to\phi_u}g(\phi)=-\infty\ . \tag{3.9}$$

The collection of thermal excitation integrals appearing in the Z_N expression (3.5) can be treated in the same asymptotic order. We can group together, and average, results for packings whose minima have energies lying within a narrow range about any preselected value $N\phi$. The corresponding

free-energy per particle f is defined by

$$f(\beta,\phi)=-\lim_{N\to\infty}(N\beta)^{-1}\ln \times\left\langle \int_{R(\alpha)}\exp[-\beta\Delta_\alpha\Phi(\vec{r})]d\vec{r}\right\rangle . \tag{3.10}$$

Just as will be the case for the coarse graining used to define g above, the width of the ϕ integral over which the average in this last equation is to be carried out can go to zero as N diverges.

In view of these asymptotic considerations the partition function expression (3.5) may be rewritten

$$Z_N\sim\lambda^{-DN}\int_{\phi_0}^{\phi_u}\exp\{N[g(\phi)-\beta\phi-\beta f(\beta,\phi)]\}d\phi . \tag{3.11}$$

It suffices to employ a maximum-integrand evaluation in Eq. (3.11) in order to obtain the system's free-energy correct to order N. In other words, if ϕ_m is the solution to

$$g(\phi)-\beta\phi-\beta f(\beta,\phi)=\max \tag{3.12}$$

for given density and temperature, then

$$\ln Z_N\sim N[g(\phi_m)-\beta\phi_m-\beta f(\beta,\phi_m)] . \tag{3.13}$$

It is worth stressing at this stage that ϕ_m is the average potential per particle that would be obtained by quenching a collection of system configurations randomly selected from the thermodynamic equilibrium state at β and the fixed density. Establishing how quenching causes the thermodynamic average potential per particle $\bar{\phi}(\beta)$ to map onto the corresponding ϕ_m for the starting temperature is one of the obvious goals of this general approach. The nature of this latter mapping through the melting transition clearly has considerable importance.

IV. TWO-DIMENSIONAL GAUSSIAN CORE SYSTEM

The Gaussian core model is defined by the potential-energy function[2]

$$\Phi(r)=\sum_{i<j}\exp(-r_{ij}^2) . \tag{4.1}$$

Using the method of molecular dynamics the classical statistical mechanics of this system has been numerically investigated in both three-dimensional[3,10,11] and two-dimensional[4] versions. We shall rely on the latter as a starting point for testing the quenching procedure advocated in the preceding sections. Specifically, $N=780$ particles are involved in our two-dimensional calculations, subject to periodic boundary conditions. The fundamental cell containing the 780 particles is rectangular, with a side ratio of $15\sqrt{3}/26 =0.999\,26\ldots$ so that an unstrained triangular array with 30 rows of 26 particles will just fit. The reduced density throughout this work has the fixed value

$$\rho^*=2^{-1/2} . \tag{4.2}$$

The single most important attribute of the $D=2$ Gaussian core model is that it exhibits a first-order melting transition. Under the fixed density condition (4.2) we have previously identified the coexistence region as[4] ($T^*=1/\beta$)

$$6.6\times10^{-3}\lesssim T^*\lesssim 7.2\times10^{-3} . \tag{4.3}$$

In the course of our simulation studies we have found that hysteresis effects (superheated crystal, supercooled fluid) could be generated by relatively rapid temperature changes through region (4.3). However, it is within the capacity of available computing power to avoid such effects with sufficiently slow temperature variation. Figure 1 shows some pressure results through the transition region calculated during one cooling and reheating se-

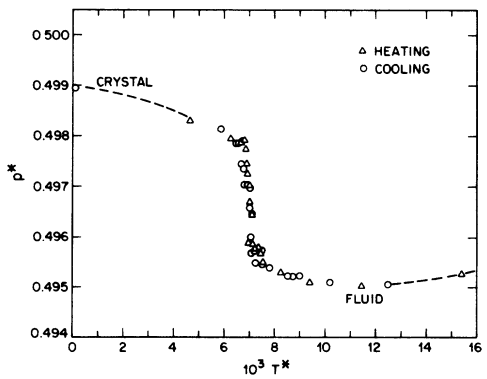

FIG. 1. Pressure vs temperature for the two-dimensional Gaussian core model. Data only from a single cooling-heating sequence are shown explicitly. Dashed curves show previous results inferred for the two pure phases. The reduced density is $3^{-1/2}$. Pressure drop upon melting is characteristic of the Gaussian core model in both two and three dimensions if the density is sufficiently high.

quence. While numerical fluctuations obviously are present it appears that substantially the same curve has been traced in both directions.

Twelve system configurations were selected and quenched. They are listed in Table I as A–L, where the thermodynamic state that supplied each one is identified. Those thermodynamic states include both crystalline and fluid cases, as well as three examples (C, D, and E) chosen from the coexistence region. We have found in the course of the molecular-dynamics study that phase coexistence is relatively easy to prepare and to maintain in this two-dimensional system.

Table II shows the potential energies achieved by quenching each of the 12 configurations. Brief descriptions are supplied for the final system structures, some details of which are discussed below (including definition of disorder parameter n_5).

Our numerical procedure for carrying out the quenching begins by solving Eq. (2.1) directly, using a fourth-order algorithm due to Gear[12] and a time increment

$$\Delta t^* = 1.25 \times 10^{-3} . \tag{4.4}$$

While it is possible to continue this integration procedure essentially to the quench end point, experience shows this to be inefficient. Thus, after an initial phase which exhibits most of the potential-energy reduction we convert to an efficient function minimization routine involving the conjugate gradient technique.[13]

By monitoring the course of the quenches from start to finish it becomes clear that complex system reorganization can be involved. Figure 2 shows for starting configuration J how the "temperature" [i.e., mean kinetic energy per particle as determined by the solution to Eq. (2.2)] varies as quenching causes Φ to decline. Instead of a simple relaxation behavior which would produce a linear curve in the given Φ vs T^* representation, a complicated meander emerges. This kind of behavior unfortunately makes the numerical contruction of quenches for the given system a rather demanding task regardless of the algorithm used, and it has severely limited the number of quenches we have been able to construct.

The assignment of nearest-neighbor polygons to particles is a convenient way to reveal and to analyze structural disorder in two-dimensional systems.[4,14] All particles inhabit hexagonal polygons in the defect-free triangular lattice that obtains at the low-temperature limit. The presence of nonhexagonal nearest-neighbor polygons (disclinations) indicates disorder. It is a topological necessity[4,14] that for any particle configuration in the system

$$\sum j n_j = 6N , \tag{4.5}$$

where n_j is the number of nearest-neighbor polygons with j sides. Thus, any disruption of the perfect triangular crystal which creates, say, a set of pentagons must compensate by simultaneously creating an appropriately weighted set of polygons having more than six sides.

Figure 3 shows configuration H (see Table I), which was selected at random from a molecular dynamics run for the homogeneous fluid phase just above its melting point. Each of the 780 particles in the fundamental cell is shown in a way which indicates how many sides its nearest-neighbor polygon possesses. For simplicity, all "sixes" have been rendered simply as asterisks. The picture

TABLE I. Configurations selected for quenching.

Name	T^*	$p^* \times 10$	$\langle \Phi \rangle$	Phase
A	4.9950×10^{-5}	4.989 470	323.480 44	Rotated crystal, two interstitials
B	1.5579×10^{-4}	4.992 581	323.395 12	Aligned crystal
C	6.9402×10^{-3}	4.957 388	330.540 26	Coexistence
D	6.9584×10^{-3}	4.968 400	329.866 29	Coexistence
E	6.9726×10^{-3}	4.964 738	330.119 34	Coexistence
F	6.9939×10^{-3}	4.954 683	330.750 20	Slightly supercooled fluid
G	7.0010×10^{-3}	4.980 190	329.179 23	Superheated aligned crystal
H	7.4083×10^{-3}	4.954 778	331.113 66	Fluid
I	8.7026×10^{-3}	4.952 711	332.342 44	Fluid
J	1.5429×10^{-2}	4.952 522	337.959 16	Fluid
K	3.4700×10^{-2}	4.995 280	351.577 43	Hot fluid
L	1.7378	14.876 84	590.599 30	Nearly ideal gas

TABLE II. Quenched configurations.

Name	Φ	n_5	Structure
A	323.442 65	4	Rotated crystal, two interstitials
B	323.273 43	0	Perfect aligned crystal
C	323.273 43	0	Perfect aligned crystal
D	323.392 98	2	Two nearby dislocations
E	323.418 00	2	Two separated dislocations
F	323.442 02	4	Rotated crystal, two interstitials
G	323.273 43	0	Perfect aligned crystal
H	324.093 27	21	Two antiparallel grain boundaries
I	323.509 46	4	Four dislocations
J	323.514 84	4	Four dislocations, slightly rotated grain
K	323.709 75	9	Two antiparallel grain boundaries
L	323.947 11	16	Enclosed grain

presented is typical of the fluid in this temperature range. While the majority of particles have six neighbors, substantial numbers have five or seven and, infrequently, cases of four or eight will be encountered. While the spatial distribution of these various coordination species is clearly inhomogeneous at any given instant, no simple description of the topological texture immediately suggests itself.

Figure 4 presents the structure that develops from configuration H in Fig. 3 as a result of quenching. The simplification produced is dramatic. The number of nonhexagonal particles drops sharply, and those that are left show a rather clear pattern of alternating five's and seven's along paths across the periodic unit cell. A close 5-7 pair of disclinations constitutes a dislocation,[4,14] and a curvilinear sequence of oriented (heat-to-tail) dislocations constitutes a grain boundary between crystalline domains.[15] The angle of rotation between neighboring domains is related to the mean separation between dislocations on the boundary. Evidently, the quenching operation has managed to reveal a polycrystalline structure that lay hidden in the starting configuration due to thermal disruption.

In all of the quenches we have carried out the final result has contained only polygons with five, six, or seven sides. The conservation condition (4.5) thence requires equal numbers of pentagons (n_5) and heptagons (n_7). We have found it convenient to classify quench packings by their n_5 values as a measure of overall disorder. These

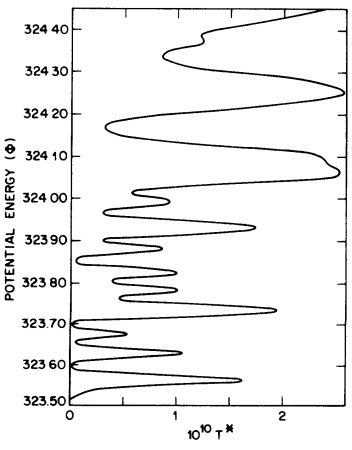

FIG. 2. Potential energy vs temperature during quench of the fluid configuration J.

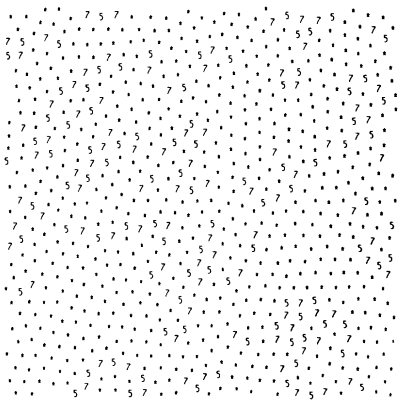

FIG. 3. Particle arrangement for configuration H. This was selected at random from the fluid just above its freezing point. Particles are classified according to nearest-neighbor polygons; asterisks imply hexagons while integers specify polygon side counts for nonhexagonal cases.

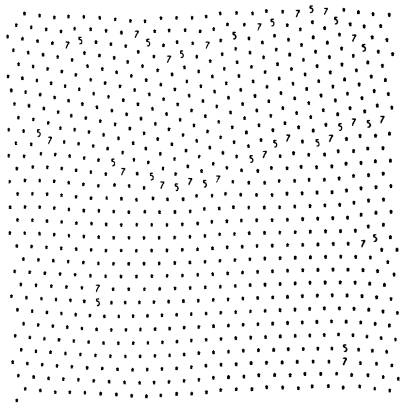

FIG. 4. Quenched structure produced from configuration H.

values have been entered in Table II.

Figure 5 exhibits the quench packing that emerges from configuration L. The starting point in this case was an extremely hot gas at about 240 times the freezing temperature. At his high temperature, particles interpenetrate deeply upon collision, and we find for this thermodynamic state that the pair-correlation function at zero separation has the value

$$g^{(2)}(r=0)=0.65\ . \tag{4.6}$$

From Fig. 5 one concludes that hidden under the nearly ideal-gas configuration is once again a polycrystalline structure. In contrast to the antiparallel pair of grain boundaries that ran across the system in the packing shown in Fig. 4, the grain boundary closes on itself to yield an enclosed crystallite in a surrounding matrix, rather than a system-spanning strip.

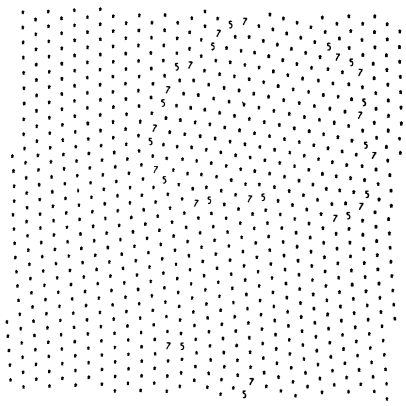

FIG. 5. Quenched structure produced from the very hot fluid configuration L.

The particle packings produced from fluid states do not always obviously have polycrystalline character. Figure 6 shows the result obtained by quenching configuration I, wherein four dislocations appear. When the slightly supercooled fluid configuration F is quenched, the result, shown in Fig. 7, consists of a rotated crystal that in defect-free form would contain 778 particles; the two excess particles are present as locally relaxed interstitials whose positions are revealed by compact 7-5-7-5 tetrads.

While the aligned perfect crystal can emerge from the positive-temperature equilibrium crystal (B), the superheated crystal (G), and even the coexistence state (C), this is not the only option. Firstly, a distinguishable (but nearly isoenergetic) crystal rotated by 90° can spontaneously form by freezing the fluid phase to the solid; subsequent quenching of the solid will only damp out phonon modes in such a structurally perfect but still rotated crystal. Secondly, there is a good chance (we estimate about $\frac{2}{3}$) that spontaneous freezing will create a misaligned solid, the quenched version of which has already been shown in Fig. 7. Whether an aligned or misaligned crystal forms in a molecular-dynamics sequence which cools the system slowly through the transition region is a matter of chance. But once the choice has been made it is very difficult for the system to convert to the other option by solid-phase annealing. Instead, it is, practically speaking, always necessary to remelt and refreeze.

Figure 8 shows the quenched structure stemming from confguration A. The latter was spontaneous-

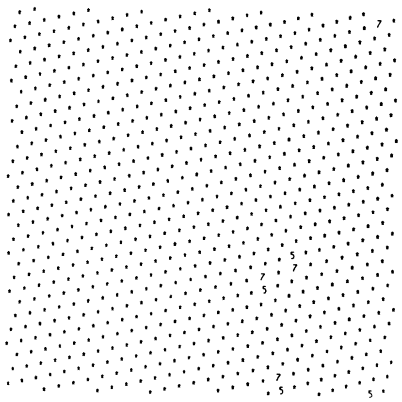

FIG. 6. Structure produced by quenching configuration I. The separated 5 and 7 disclinations at lower- and upper-right corners are actually neighbors due to the periodic boundary conditions.

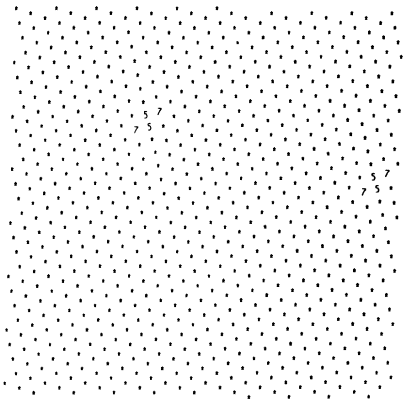

FIG. 7. Rotated crystal containing two interstitials that is produced by quenching supercooled fluid configuration F.

ly frozen by slow cooling from the homogeneous fluid, and was then cooled in stages to its thermodynamic temperature listed in Table I. The structure shown in Fig. 8 has the same misaligned $N=778$ crystal character as that shown earlier in Fig. 7. However, now the two interstitials have come to rest in a slightly different position with slightly higher energy. Evidently, there is a band of energies corresponding to various stable arrangements of the interstitials, for each one of which there is a distinct configuration-space region $R(\alpha)$.

It is obvious that hidden structure uncovered by quenching should produce sharpening of the molecular distribution function. Figure 9 shows the pair-correlation functions $g^{(2)}(r)$ before and after the quench of configuration H. The lower curve is simply the smooth function appropriate to the equilibrium fluid at a reduced temperature T^* of approximately 7.41×10^{-3}. In principle, the upper curve should consist of a discontinuous sum

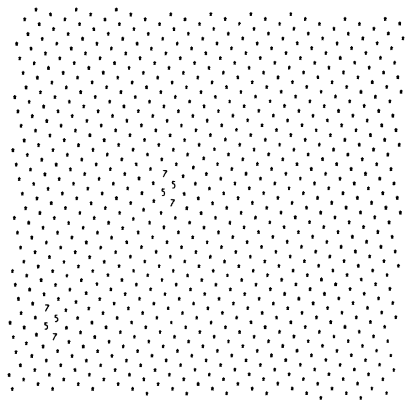

FIG. 8. Quenched configuration produced from configuration A in Table I.

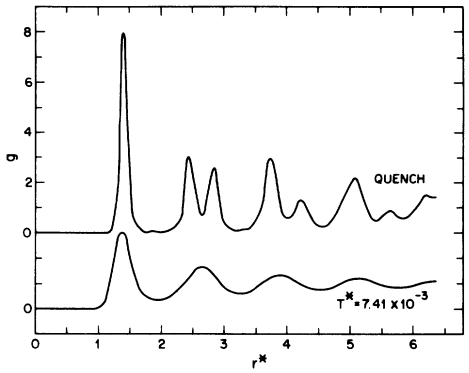

FIG. 9. Pair-correlation functions for fluid at $T^*=7.41\times10^{-3}$ and the corresponding quench (from configuration H).

of closely spaced Dirac δ functions since all 780 particles are strictly at rest. However, data were collected in bins of radial width Δr^* equal to 0.08, and we show only the corresponding smoothed curve. Even so, the sharpening of peaks upon quenching is very clear. Successive peaks in the quench function correlate strongly with those that have been calculated before for the low-temperature crystal,[4] but increasing peak width with increasing r^* arises now from built-in strain due to dislocations, not to phonon motion. The sharpness of the quench $g^{(2)}$'s correlates inversely with the parameter n_5 listed for each case in Table II.

The quench energies are plotted against the corresponding n_5 values in Fig. 10. The smooth curve shown represents the function

$$H(n_5)=\Phi_0+An_5+B-(B^2+C^2n_5^2)^{1/2}\,, \tag{4.7}$$

where

$$\Phi_0=323.27343 \tag{4.8}$$

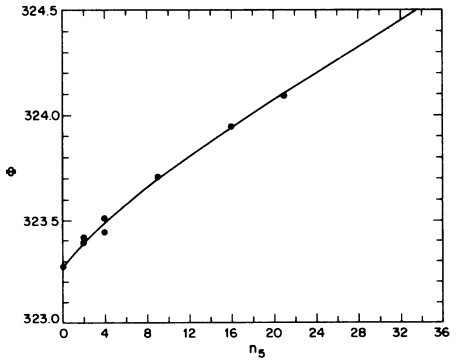

FIG. 10. Potential energy of the quenched configuration vs n_5. The smooth curve is specified in Eq. (4.7).

is the potential energy of the perfect crystal, and where constants A, B, and C were obtained by a least-squares fit:

$$A = 0.0623 ,$$
$$B = 0.2145 , \tag{4.9}$$
$$C = 0.0314 .$$

The rms deviation is 2.723×10^{-2} for the points with $n_5 > 0$. One sees from Fig. 10 that on the average the potential energy of the quenched packings rises with n_5. But the downward curvature illustrated with the smooth-fit function H implies that dislocations soften the crystal and tend to make it easier to insert yet further dislocations. It may be noted that $H'(0)$ is over twice as large as the limiting slope of this function for large n_5.

Although the small number of quenches actually carried out makes such inferences risky, we believe that ϕ_m increases only by about 2×10^{-4} across the melting transition. This is a rather small fraction of the latent heat change per particle 2.1×10^{-3}. The remainder must be attributed to increasing anharmonicity.

V. DISCUSSION

Even though we have been able to investigate only a modest number of quenched configurations, several conclusions can be drawn. Most important, perhaps, is that the correlation length in the random packings generated (i.e., the mean diameter of crystalline grain regions and/or the mean separation of isolated dislocations) is comparable to the size of the system used. This causes the quench energies to scatter rather widely, making it difficult to extract ϕ_m accurately from our results. In order to avoid such scatter it may be necessary to employ two-dimensional systems of at least 10^4 particles and/or to perform many more quenches.

The large correlation length present in the quench structures probably reflects a general sparseness of stable packings in two dimensions, compared to three dimensions. In the one-dimensional case there is only one packing, the regular periodic array; two dimensions permits a limited diversity of packings with, at most, a rather low concentration of disorder elements (disclinations). It is reasonable to suppose that for fixed N the number of distinct packings continues to increase with dimension beyond two.

The structure presented earlier in Fig. 5 shows that large correlation lengths arise even when one starts the quench with the very high-temperature fluid. It seems obvious that the correlation lengths in all thermodynamic fluid states are bounded from above by the corresponding quench correlation lengths.

The presence of the boundaries for the multidimensional regions $R(\alpha)$ makes it unlikely that a system confined to any one such region could undergo a melting transition.[16] Rather, it should be the shift from low-disorder $R(\alpha)$'s to higher-disorder $R(\alpha)$'s that characterizes melting. A corollary statement is that for fixed ϕ the free-energy function $f(\beta,\phi)$ [Eq. (3.10)] will be analytic in β throughout the transition region of this variable. The nonanalytic character of the phase transition then resides in the quantity ϕ_m as a function of β. The Appendix supports this viewpoint with a simple (and crude) estimation of the partition function that predicts the existence of the first-order melting transition.

Clearly, it is desirable to apply the quench procedure to three-dimensional systems to see what type of hidden order emerges. If our presumption is correct that three dimensions permit many more random packings and that they have shorter correlation lengths, then useful and reproducible results should be attainable with reasonable system sizes ($N < 10^3$). For the case of monatomic substances in three dimensions, one potentially valuable way to classify random packings (in addition to using nearest-neighbor polyhedra) would be to follow Rivier's procedure for identifying disclination lines.[17]

Great interest also surrounds the study of polyatomic substances in three dimensions. The case of water is particularly important in regards to the hydrogen bond topology of its quenches from the stable liquid state.[18] Specifically, one would seek to identify local regions similar in structure to the known ices[19] or clathrate hydrate crystals.[20] In addition it might be useful to examine quenches of strongly supercooled liquid water, since emergence of hidder order could help to explain the supercooling anomalies that appear to exist at approximately -45 C.[21]

We express thanks to Dr. Linda Kaufman of Bell Telephone Laboratories for suggesting the "conjugate gradient method" which leads to drastic improvement in convergence rate for the quench procedure, and for providing the necessary computer software.

APPENDIX

We now show how the preceding observations on the Gaussian core model can be assembled into a "theory" of the first-order melting transition. We begin by accepting the fitting function shown in Fig. 10 and Eq. (4.7) as a proper description (in the large system limit) for packing energies with various degrees of disorder. For present purposes it is most convenient to rewrite H in a form which makes its extensive character explicit:

$$H(n_5)=N[\phi_0+Ax_5+b-(b^2+C^2x_5^2)^{1/2}] \equiv N\phi(x_5) . \tag{A1}$$

Here we have set

$$x_5=n_5/N ,$$
$$\phi_0=\Phi_0/780=0.414\,453 , \tag{A2}$$
$$b=B/780=2.750\times10^{-4} .$$

The parameters A and C were specified earlier in Eq. (4.9).

In estimating the number of distinct packings that can be formed when precisely $n_5=Nx_5$ pentagonal disclinations exist in the N-particle system, we must keep in mind that the disclinations typically must be arranged in linear grain boundaries with some average separation. In laying down a grain boundary across an initially defect-free system one can reckon that on average some number E of choices will exist at each stage for lengthening the boundary by one 5-7 disclination pair. On this basis E^{n_5} would be the appropriate estimate for the total number of n_5 packings. But the fact is that grain boundaries can interfere with one another, requiring a reduction in this estimate for large n_5 (i.e., large x_5). This is borne out by the fact that our numerical procedure above fails to produce packings with high defect concentrations (x_5 approaching $\frac{1}{2}$).

Consequently, we postulate a linear reduction with x_5 in the factor E. The modified estimate for the number of packings at fixed n_5 is thus taken to be

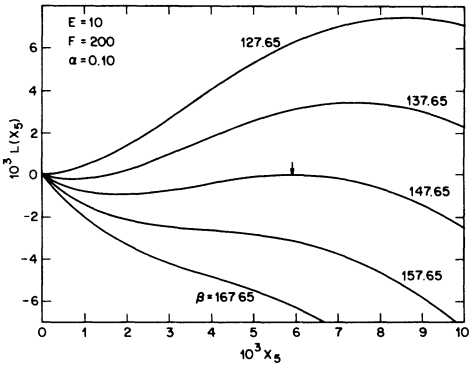

FIG. 11. Graphical determination of the integrand maximum in Eq. (A7). Below the melting point ($\beta > 147.65$), x_5 sticks at the origin; above the melting point ($\beta < 147.65$), x_5 has discontinuously jumped to the position of a new maximum.

$$(E-Fx_5)^{Nx_5} , \tag{A3}$$

where E and F are suitable positive constants.

Next, we need an expression for the vibrational free-energy function $f[\beta,\phi(x_5)]$. When x_5 vanishes so the perfect crystal obtains, the free-energy is indeed attributable to harmonic phonon modes $\omega_j^{(0)}$ at low temperature; hence,

$$\exp[-N\beta f(\beta,\phi_0)]=\sum_{j=1}^{2N}(\beta\hbar\omega_j^{(0)})^{-1} . \tag{A4}$$

Normal modes ω_j in defective packings will differ from the crystal $\omega_j^{(0)}$, obviously. We suggest that the predominant effect stems from the defect softening of the medium conveyed by downward curvature of $H(n_5)$. The derivative H' provides a measure of the rigidity of the medium, and it seems reasonable that at least *some* of the normal modes (principally, those of low frequency and of shear character) ought to be rescaled by a softening factor

$$[H'(0)/H'(Nx_5)]^{1/2} . \tag{A5}$$

If we let α stand for the fraction of modes subject to this rescaling, then

$$\exp\{-N\beta f[\beta,\phi(x_5)]\}\simeq\left[1-\frac{C^2x_5}{A(b^2+C^2x_5^2)^{1/2}}\right]^{-\alpha N}\prod_{j=1}^{2N}(\beta\hbar\omega_j^{(0)})^{-1} . \tag{A6}$$

These expressions can be used to provide an approximate expression for the partition function Z_N along the lines indicated earlier by Eq. (3.11). In that representation ϕ was treated as the fundamental intensive variable, but in view of Eq. (A1) we can transform to x_5 as the more convenient choice. By using expressions (A1), (A3), and (A6) we arrive at the following expression for Z_N:

$$Z_N \simeq N\lambda^{-2N}\exp\{-N\beta[\phi_0+f(\beta,\phi_0)]\}$$
$$\times\int_0^{E/F}dx_5\exp\{-N\beta[Ax_5+b-(b^2+C^2x_5^2)^{1/2}]\}(E-Fx_5)^{Nx_5}\left[1-\frac{C^2x_5}{A(b^2+C^2x_5^2)^{1/2}}\right]^{-\alpha N}. \tag{A7}$$

In the large-N limit the free-energy per particle will be determined by that value of x_5 which maximizes the integrand. Equivalently, we require that x_5 at each β which satisfies

$$L(x_5)=x_5\ln(E-Fx_5)-\alpha\ln\left[1-\frac{C^2x_5}{A(b^2+C^2x_5^2)^{1/2}}\right]-\beta[Ax_5+b-(b^2+C^2x_5^2)^{1/2}]=\max . \tag{A8}$$

Three unevaluated parameters appear in the last equation: E, F, and α. We now see that choices for each that are probably reasonable lead to a prediction of a first-order melting transition. In particular, we select

$$E=10\ ,\quad F=200\ ,\quad \alpha=0.10\ . \tag{A9}$$

The first of these asserts that on the average, ten choices exist for extending a grain boundary by a 5-7 pair in a pristine medium. The second then states that random packings become negligibly rare when the fractional disclination density x_5 reaches 0.05. The α value shown subjects only a small fraction of the normal modes to the full softening effect.

Figure 11 shows $L(x_5)$ curves vs x_5 for several choices of the temperature parameter β. When $\beta>147.65$ the curves monotonically decline with increasing x_5 from their maximum value 0 at the origin. However, when $\beta<147.65$, $L(x_5)$ achieves its greatest value at a local maximum displaced to positive x_5. There is thus a discontinuity at the melting point

$$\beta=147.65\ ,\qquad T^*=1/\beta=6.7728\times10^{-3}\ , \tag{A10}$$

at which the integrand-maximizing value of x_5 jumps from 0 (low-temperature crystal) to 5.918×10^{-3} (fluid at the transition point). For continued temperature increase the local maximum continues to predominate, finally approaching the x_5 value 3.065×10^{-2} at infinite temperature.

That the predicted melting temperature (A10) agrees well with the one determined by molecular dynamics for the Gaussian core model [Eq. (4.3)] primarily results from adroit choice of α. However, the mean value predicted for n_5 in quenches from the $N=780$ fluid at its freezing point,

$$\langle n_5\rangle=4.612\ , \tag{A11}$$

seems roughly correct in comparison with entries displayed in Table II.

The latent heat predicted for the transition is 0.0461 with the parameter set (A9). This is too large by a factor of approximately 2, but doubtless agreement could be improved by varying α, E, and F.

It is important to stress that the predicted existence of a first-order transition rests fundamentally on the nonlinearity with x_5 of the function H. That is, the softening phenomenon appears to be a prerequisite, and paves the way for an avalanche of defects to enter the system at the transition point.

Of the major deficiencies of the present simple view of constant-density melting is that it fails to produce a coexistence interval [see Eq. (4.3) above], as is required when the densities of the equal-pressure phases differ. Correcting this would require accounting for correlation of density fluctuations with disclination concentration fluctuations in the stable packings. It is worth pointing out in this connection, however, that at one special density for the Gaussian core model the molar densities are equal and the coexistence interval shrinks to a point.

[1]An outline of some of the ideas presented here has been previously published: F. H. Stillinger and T. A. Weber, Kinam 3A, 159 (1981).
[2]F. H. Stillinger, J. Chem. Phys. 65, 3968 (1976).
[3]F. H. Stillinger and T. A. Weber, J. Chem. Phys. 68, 3837 (1978); 70, 1074(E) (1979).
[4]F. H. Stillinger and T. A. Weber, J. Chem. Phys. 74, 4105 (1981); 74, 4020 (1981).
[5]B. I. Halperin and D. R. Nelson, Phys. Rev. Lett. 41, 121 (1978); 41, 519(E) (1978).
[6]D. R. Nelson and B. I. Halperin, Phys. Rev. B 19, 2457 (1979).
[7]G. Jacucci (private communication).
[8](a) A. C. Belch, S. A. Rice, and M. G. Sceats, Chem. Phys. Lett. 77, 455 (1981); (b) F. Hirata and P. J. Rossky, J. Chem. Phys. 74, 6867 (1981).
[9]S. A. Rice, Top. Curr. Chem. 60, 109 (1975).
[10]F. H. Stillinger and T. A. Weber, J. Chem. Phys. 70, 4879 (1979).
[11]F. H. Stillinger and T. A. Weber, Phys. Rev. B 22, 3790 (1980).
[12]C. W. Gear, Argonne National Laboratory Report No. ANL-7126 (unpublished).
[13]R. Fletcher, *Practical Methods of Optimization* (Wiley, New York, 1980).
[14]J. P. McTague, D. Frenkel, and M. P. Allen, in *Ordering in Two Dimensions,* edited by S. K. Sinha (Elsevier-North-Holland, New York, 1980), pp. 147-151.
[15]W. T. Read and W. Schockley, Phys. Rev. 78, 275 (1950).
[16]For particles with attractive forces, however, confinement to an $R(\alpha)$ many not be sufficient to inhibit a vaporization transition if the overall system density is small.
[17]N. Rivier, Philos. Mag. A40, 859 (1979).
[18]A. Rahman and F. H. Stillinger, J. Am. Chem. Soc. 95, 7943 (1973).
[19]N. H. Fletcher, *The Chemical Physics of Ice* (Cambridge University Press, Cambridge, 1970), Chaps. 2 and 3.
[20]D. W. Davidson, in *Water, A Comprehensive Treatise,* edited by F. Franks (Plenum, New York, 1973), Vol. II, pp. 115-234.
[21]C. A. Angell, in *Water, A Comprehensive Treatise,* edited by F. Franks (Plenum, New York), Vol. VII (to be published).